

## GEOTHERMAL CORROSION OF IRON AND STEEL

B.G. Pound, G.A. Wright and R.M. Sharp\*

Chemistry Department,  
 \*Chemical and Materials Engineering Department,  
 University of Auckland.

## ABSTRACT

The corrosion of iron and carbon steel in geothermal condensates is being studied using electrochemical techniques. The anodic oxidation of iron in simulated geothermal condensates (deaerated) produces a black solid which has been identified by x-ray diffraction as the iron sulphide, mackinawite,  $\text{Fe}_{1+x}\text{S}$ . The mackinawite readily spalls from the metal, giving rise to a steady corrosion rate with time of both iron and carbon steel in condensates.

The cathodic process in these deaerated condensates occurs by the reduction of  $\text{H}_2\text{S}$  to  $\text{H}_2$ . The reduction mechanism involves adsorbed hydrogen atom intermediates which react to form hydrogen molecules. Potential step transients and a.c. impedance methods have been used to investigate the behaviour of the adsorbed hydrogen atoms. The surface concentration of  $\text{H}(\text{ads})$  has been measured and it is shown that some of the adsorbed hydrogen dissolves in the metal.

## INTRODUCTION

The use of a particular metal in contact with geothermal fluids is influenced by the nature of the corrosion products and by hydrogen ingress into the metal. The formation of a protective surface film on a metal giving rise to low corrosion rates is highly desirable. However, hydrogen ingress which is a major factor in the embrittlement of various steels can be a severe problem. In order to examine these factors, the corrosion behaviour of iron and carbon steel in geothermal condensates is currently under investigation using a variety of electrochemical methods.

## ANODIC REACTIONS

The anodic oxidation reaction in the corrosion process and the surface films produced depend on both the potential of the metal and the nature of the corrosive medium. The potential regions in which the anodic and cathodic reactions occur can be found from cyclic voltammograms, obtained by linearly sweeping the potential of the test metal and following the current response.

The cyclic voltammogram of iron (Pound et al., 1979) in an aqueous solution containing NaCl and

$\text{NaHCO}_3$  is shown in Figure 1. As the potential of the iron is scanned in the positive direction, a film of oxide forms on the surface. This process is indicated by the shoulder, A, in the anodic current and the large cathodic peak which corresponds to subsequent reduction of the film.

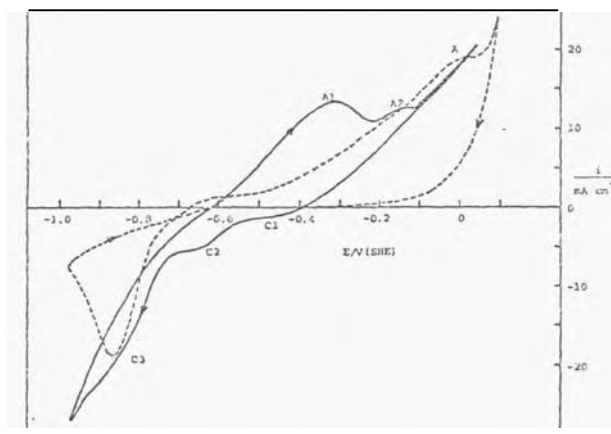


Figure 1. Cyclic voltammogram of iron in a solution containing NaCl and  $\text{NaHCO}_3$ .  
 $(\text{Cl}^-) = 0.032 \text{ mol/l}$ .  
 $(\text{HCO}_3^-) = 0.003 \text{ mol/l}$ .  
 ----- No  $\text{H}_2\text{S}$ , ———  $\text{H}_2\text{S}$  present  
 $(0.055 \text{ mol l}^{-1}, \text{pH} = 5.8)$ .  
 Potential sweep rate =  $100 \text{ mV s}^{-1}$ .

The sharp increase in current following A corresponds to a breakdown of the film; pitting occurs and passivation of the iron does not take place. When the direction of the potential sweep is reversed, higher currents result as shown in Figure 2, signifying that the pits continue to grow. Eventually pit growth is reduced and the current exhibits a steep decrease. The role of chloride in the pitting of metals is well documented and the occurrence of pitting on iron in the  $\text{Cl}^-/\text{HCO}_3^-$  solution is therefore to be expected. A scanning electron microscope examination of the iron confirmed that pits had formed extensively over the surface.

In the presence of  $\text{H}_2\text{S}$ , the anodic reactions on iron occur at higher rates as apparent from Figure 1. A black solid product which was

Pound, et al.

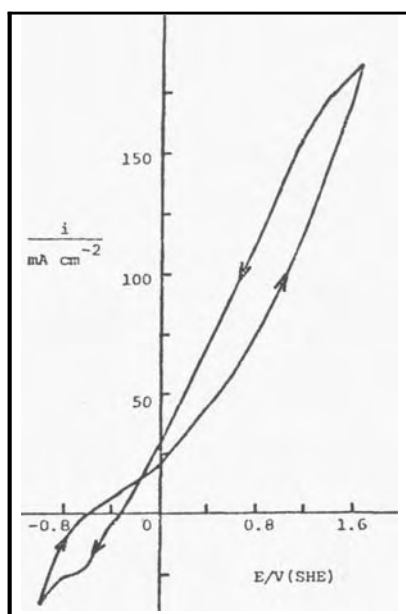
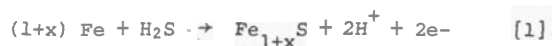


Figure 2. Cyclic voltammogram showing pitting region of iron.  
Solution composition as indicated in Figure 1.  
Potential sweep rate =  $100 \text{ mV s}^{-1}$ .

identified by x-ray diffraction as the iron sulphide, mackinawite, is formed in the potential ranges of A1 and A2 (Figure 1) according to the reaction:



The mackinawite is non-adherent and readily spalls from the metal surface. The lack of protection afforded to the iron by the loose mackinawite film results in approximately constant corrosion rates with time for iron and carbon steel in solutions containing  $\text{H}_2\text{S}$ . Despite the high loss of material, a thin film of the sulphide remains on the iron and is available for reduction back to iron at sufficiently negative potentials. The cathodic reduction of the mackinawite gives rise to the series of arrests, C1-C3, observed in the cyclic voltammogram.

Corrosion products can be predicted from potential-pH diagrams if the pH and electrode potential are known. A potential-pH diagram for the  $\text{Fe/S/H}_2\text{O}$  system is shown in Figure 3. The potential at which  $i = 0$  on the forward sweep in the cyclic voltammogram corresponds to the corrosion potential,  $E_{\text{corr}}$ , of iron in the  $\text{H}_2\text{S}$ -solution. The value of  $E_{\text{corr}}$  is  $-0.62 \text{ V}$  which lies in the FeS (troilite) region of stability of the potential-pH diagram. Since mackinawite is known (Berner, 1967) to be thermodynamically unstable relative to troilite, it is concluded that mackinawite is a meta-stable reaction product whose appearance is controlled by kinetic factors rather than thermodynamics.

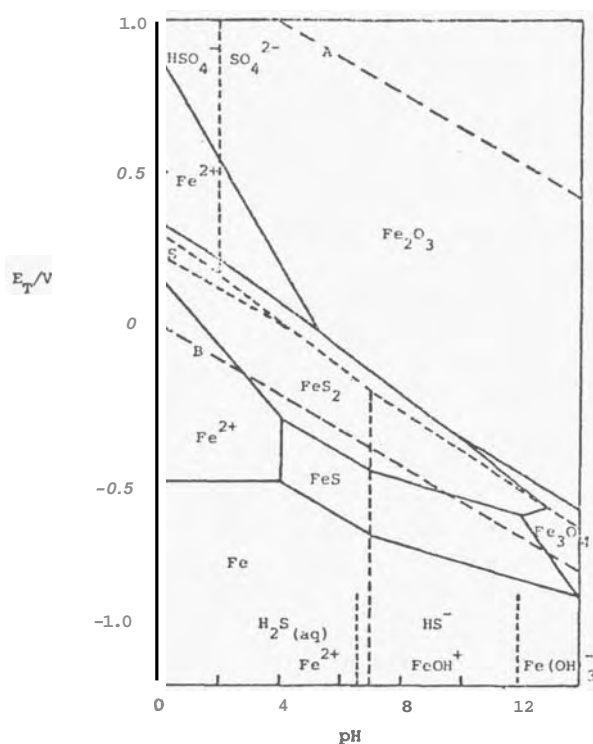
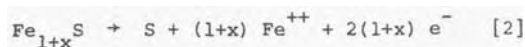


Figure 3. Potential-pH diagram for  $\text{Fe/S/H}_2\text{O}$  System at 298 K.  
The conditions selected apply to cold condensate at the Broadlands Corrosion Test Rig operated by D.S.I.R.  
 $(\text{Fe}^{2+}) = 10^{-4} \text{ mol l}^{-1}$ ,  
 $(\text{H}_2\text{S} + \text{HS}^-) = 10^{-3} \text{ mol l}^{-1}$   
Line B represents the equilibrium  $\text{H}_2/\text{H}^+$  for 101 kPa hydrogen pressure, and Line A represents the  $\text{H}_2\text{O}/\text{O}_2$  equilibrium for 101 kPa oxygen pressure (but  $\text{O}_2$  is normally absent or present only in trace amounts).  $\text{S}^{2-}$  was not considered since experimental evidence (Ellis and Giggenbach, 1971) indicates that its existence is unlikely in aqueous solutions.

Mackinawite itself was electrochemically oxidised (Pound et al., 1980) in the absence of  $\text{H}_2\text{S}$  using a carbon paste electrode. The paste consisted of a finely ground mixture of mackinawite and graphite in 10 mol/l ammonium acetate solution. In principle, this type of electrode allows most of the solid to undergo reaction because of the close contact with the electron-conducting graphite.

The potential sweep curve for the anodic oxidation of mackinawite is shown in Figure 4. Two oxidation steps are observed and an x-ray diffraction examination identified sulphur as the dominant product at both peaks. The conversion of mackinawite can be considered to proceed according to the reaction:



in which the formation of sulphur evidently takes place on the surface of the iron sulphide particles. The second oxidation peak appears to correspond to a reactivation of the sulphur-forming reaction, possibly due to a change in the composition of the underlying iron sulphide.

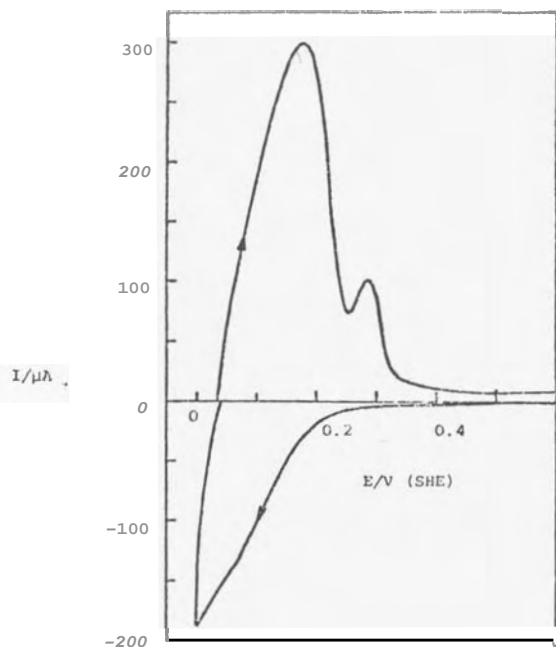
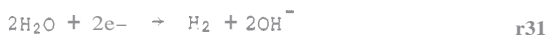


Figure 4. Oxidation of mackinawite at the carbon paste electrode. Potential sweep at 0.1 mV/s using 1 mg  $\text{Fe}_{1+x}\text{S}$  + 30 mg graphite (particles 30 to 50  $\mu\text{m}$ ) in 10 mol  $\text{l}^{-1}$   $\text{NH}_4\text{OOCCH}_3$  at 20°C.

#### CATHODIC REACTIONS

In a neutral, deaerated solution in the absence of  $\text{H}_2\text{S}$ , the cathodic reaction involves the evolution of hydrogen.



When  $\text{H}_2\text{S}$  is present, hydrogen is formed by the reduction of  $\text{H}_2\text{S}$  (Bolmer, 1965).



giving rise to an increased cathodic current as shown in Figure 1. Stirring of the solution promotes the transport of  $\text{H}_2\text{S}$  to the iron surface and thereby causes a substantial increase in the current. It can be seen from Figure 1 that the hydrogen-evolution current also depends on the potential applied to the iron. Potential-step experiments have established that the rate of  $\text{H}_2\text{S}$  reduction is controlled partly by the transfer of charge and partly by the diffusion of  $\text{H}_2\text{S}$  to the metal surface.

By measuring the a.c. impedance of iron in

$\text{H}_2\text{S}$ -solutions over a wide range of frequencies, it was shown that the formation of hydrogen by reaction [4] involves adsorbed hydrogen atoms,  $\text{H}(\text{ads})$ . The reaction mechanism is then as follows:



The presence of  $\text{H}(\text{ads})$  on iron was examined by use of an anodic potential-step technique in which the charge,  $Q_A$  (Figure 5), passed was attributed to the oxidation of adsorbed hydrogen. At sufficiently negative potentials,  $Q_A$  is greater than that expected for a monolayer of adsorbed hydrogen on the iron surface. It is assumed that some  $\text{H}(\text{ads})$  dissolves in the metal to form interstitial hydrogen atoms which diffuse into the bulk metal. The excess charge is then associated with the oxidation of these atoms after they diffuse back to the surface. Present experiments involve the generation of hydrogen at a known rate for a controlled time interval before stepping to the corrosion potential. The subsequent rate of oxidation is then followed as a function of time from which the time dependence of the diffusion rate of hydrogen in the bulk metal can be examined. Undoubtedly, some hydrogen remains trapped in the metal at grain boundaries and dislocations, where it can be an embrittling agent.

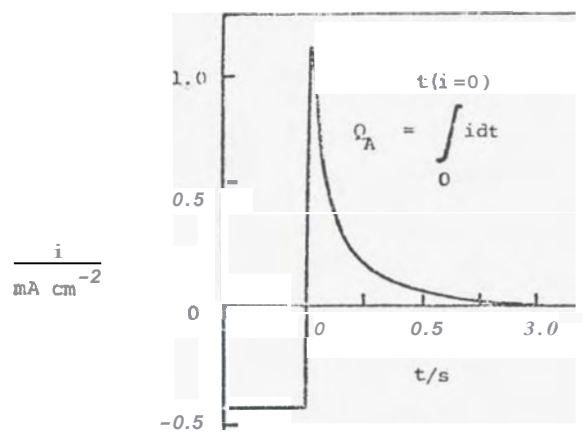


Figure 5. Current-time transient for the oxidation of  $\text{H}(\text{ads})$ . Hydrogen was formed at -750 mV (SHE) for 20 s and then the electrode potential was stepped to -620 mV (SHE). Solution composition as in Fig. 1, with 0.06 mol/l  $\text{H}_2\text{S}$ ,  $Q_A = 0.4 \text{ mC cm}^{-2}$  which is equivalent to  $2.7 \times 10^{15} \text{ H}(\text{ads}) \text{ cm}^{-2}$ .

#### ACKNOWLEDGEMENT

The authors are grateful to the N.Z. Energy Research and Development Committee for funding this project. We would also like to thank members of the Industrial Processing Division,

Pound, et al.

D.S. I.R. for their co-operation.

#### REFERENCES

- Pound, B.G., Sharp, R.M. and Wright, G.A., 1979-1980. Geothermal Corrosion Parts 1 to 7: Progress reports to New Zealand Energy Research and Development Committee, University of Auckland.
- Berner, R.A., 1967. Thermodynamic Stability of Sedimentary Iron Sulphides. *Am. J. Sci.*, V.265, p.773-785.
- Bolmer, P.W., 1965. Polarisation of Iron in  $H_2S$ -NaHS Buffers. *Corrosion*, V.21, p.69-75.
- Ellis, A.J. and Giggenbach, W., 1971. Hydrogen sulphide ionisation and sulphur hydrolysis in high temperature solution. *Geochim. et Cosmochim. Acta.*, V.35, p.247-260.